Chemical Science

ROYAL SOCIETY OF CHEMISTRY

EDGE ARTICLE

View Article Online
View Journal | View Issue

Cite this: *Chem. Sci.*, 2024, **15**, 8750

All publication charges for this article have been paid for by the Royal Society of Chemistry

Received 20th February 2024
Accepted 18th April 2024

DOI: 10.1039/d4sc01208a

rsc.li/chemical-science

β-Terrecyclene synthase constructs the quadrane backbone in terrecyclic acid biosynthesis†

Yongxiang Song,[abcd] Wengui Wang,[f] Jiafan Yang,[abc] Dewei Gao,[d] John M. Billingsley,[d] Songtao Wang,[abc] Yiguang Zhu,[abcd] Junfeng Wang,[abcd] Jianhua Ju,[ac] Yan Yan *[abcd] and Yi Tang[de]

Quadrane sesquiterpenes featuring a distinctive tricyclic skeleton exhibit potent antimicrobial and anticancer activities. Although extensive studies have attempted to reveal the multistep carbocation rearrangement involved in the formation of the tricyclic quadrane scaffold, the exact biosynthetic pathway and chemical logic to generate the quadrane structure remains mysterious. Here we identified a novel sesquiterpene synthase that is capable of generating β-terrecyclene possessing the quadrane scaffold and characterized the biosynthetic pathway of a representative fungal quadrane terrecyclic acid. Further mutagenesis coupled with isotopically sensitive branching studies of this β-terrecyclene synthase provided insight into the mechanism involved in the formation of the quadrane scaffold.

Introduction

Terpenes feature tens of thousands of structurally diverse entities and comprise the largest group of natural products. The structural complexity is generated by terpene cyclases (TCs) using linear oligo-isoprenoid diphosphate precursors including geranyl, farnesyl, geranylgeranyl, and geranylfarnesyl diphosphate.[1,2] The TCs are capable of catalyzing the most complex multistep carbocation rearrangement in nature, in which the bonding, hybridization, and stereochemistry of the substrate's carbon atoms are dramatically altered to accomplish the intriguing scaffolds. Among these structurally diversified scaffolds, quadranes belong to a family of naturally occurring sesquiterpenes consisting of a cyclopentane fused with a bicyclo[3.2.1]octane moiety (Fig. 1).[3] The first quadrane was discovered as (−)-quadrone (**1**) from the mold *Aspergillus terreus* in 1978,[4,5] which was shown to be derived from (+)-terrecyclic acid A (**2**) through an intramolecular oxa-Michael addition reaction.[6] In the past two decades, six new quadranoids were isolated from terrestrial fungi, which include (−)-8-hydroxyquadrone (**3**), terrecyclol (**4**), (−)-isoquadrone (**5**), (+)-6-hydroxyisoquadrone (**6**), (+)-5(6)-dihydro-6-hydroxyterrecyclic acid (**7**) and (+)-5(6)-dihydro-6-methoxyterrecyclic acid (**8**).[3] Interestingly, molecules possessing this unique quadrane scaffold were also discovered

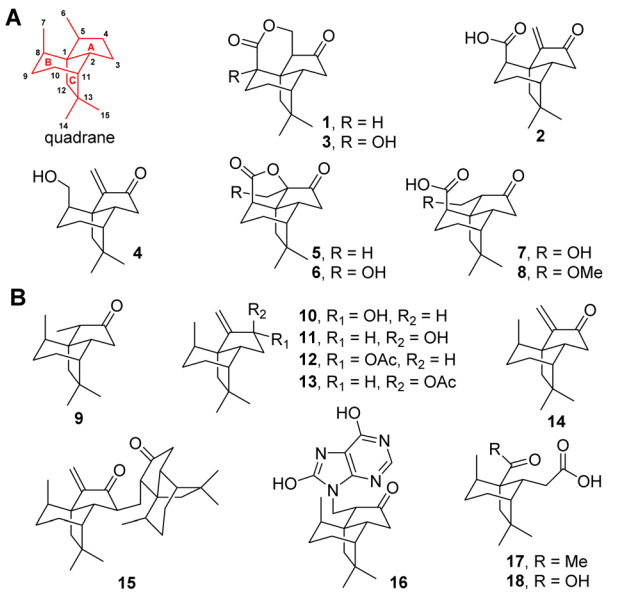

Fig. 1 Naturally occurring quadrane sesquiterpenes from fungi (A) and coral (B). The tricyclic quadrane scaffold is shown in red.

[a]*Key Laboratory of Tropical Marine Bio-resources and Ecology, Guangdong Key Laboratory of Marine Materia Medica, Innovation Academy of South China Sea Ecology and Environmental Engineering, South China Sea Institute of Oceanology, Chinese Academy of Sciences, 164 West Xingang Road, Guangzhou 510301, China. E-mail: yyan@scsio.ac.cn*

[b]*Sanya Institute of Oceanology Eco-Environmental Engineering Yazhou Scientific Bay, Sanya, 572000, China*

[c]*University of Chinese Academy of Science, 19 Yuquan Road, Beijing 100049, China*

[d]*Department of Chemical and Biomolecular Engineering, University of California, Los Angeles, CA 90095, USA*

[e]*Department of Chemistry and Biochemistry, University of California, Los Angeles, CA 90095, USA*

[f]*School of Chemistry and Chemical Engineering, University of Jinan, 336 West Road of Nan Xinzhuang, Jinan 250022, China*

† Electronic supplementary information (ESI) available: Details regarding general materials and methods, construction of strains *S. cerevisiae* and *A. nidulans*, fermentation, isolation, structure elucidation, synthetic procedures, biochemical analysis, X-ray crystallography, NMR data and NMR spectra. CCDC 2271713 and 2271714. For ESI and crystallographic data in CIF or other electronic format see DOI: **https://doi.org/10.1039/d4sc01208a**

in soft corals as(−)-suberosanone (**9**), (−)-suberosenol A (**10**), (−)-suberosenol B (**11**), (−)-suberosenol A acetate (**12**), (−)-suberosenol B acetate (**13**), (+)-suberosenone (**14**), the intermolecular Michael addition adduct of **14** as (+)-alertenone (**15**), the 7*H*-purine-6,8-diol aza-Michael addition adduct 6-(9′-purine-6′,8′-diolyl)-2β-suberosanone (**16**), ring A opened derivatives (−)-isishippuric acid A (**17**) and (−)-isishippuric acid A (**18**).[3]

Due to the potent antimicrobial and anticancer activities, the challenging construction of the quadrane scaffold has attracted considerable attention from synthetic chemists.[3,7,8] Incorporation of isotopically labeled acetate and mevalonate into the biosynthesis of **1** and **2** has revealed that quadranoids are sesquiterpenes resulting from multiple rearrangement reactions.[9–11] Based on the altered connectivities of each atom in **1** as compared to the farnesyl diphosphate (FPP) precursor, two distinct possible mechanisms known as Hirota's route[12,13] and Coates' route,[14] respectively were hypothesized to explain the multistep cascade of carbocation rearrangements involved in the formation of the tricyclic quadrane scaffold (Scheme 1). Hirota's route represents the earliest proposed mechanism involving head-to-tail cyclization of FPP to yield the monocyclic humulyl cation (**19**), which is subsequently converted to a 5/8-bicyclic carbocation intermediate (**20**) (Scheme 1A). Then rearrangement of **20** takes place to form a tricyclic intermediate (**21**), which undergoes a 1,2-hydride shift to generate **22**, and then a 1,2-alkyl shift to give **23** (Scheme 1A). Lastly, a 1,3-hydride shift leads **23** to terrecyclanyl cation **24**, which is subsequently converted into β-terrecyclene (**25**) *via* deprotonation (Scheme 1A).

In 1992, Coates proposed an alternative route based on the observation that silphinenyl cation (**30**) was readily transformed into the terrecyclanyl cation (**24**) which could be further deprotonated to give α-terrecyclene during solvolytic rearrangement (Scheme 1B).[15] The difference between these two hypotheses is the rearrangement process during the transformation of **19** into **24** (Scheme 1A). In Coates' route, monocyclic **19** is converted into caryophyllenyl ion **26**, which is followed by a 1,2-alkyl shift to generate the 5/8-bicyclic intermediate **27** (Scheme 1A). Then a carbocation rearrangement leads **27** to a tricyclic intermediate **28**, which is transformed into presilphiperfolan-8-yl ion (**29**) *via* a 1,3-hydride shift. **30** is then formed *via* a 1,2-alkyl shift of **29**, and then another 1,2-alkyl shift takes place to yield **24** (Scheme 1A).

Although Hirota's route seems unlikely since the formation of transition states of two critical steps (**22** → **23** → **24**) require high energy according to a computational study,[16] no TC catalyzing the direct conversion of FPP into **25** or α-terrecyclene had been reported, and the formation of the quadrane scaffold could also result from rearrangement of other terpene scaffolds using tailoring enzymes. Therefore, the biosynthesis of the quadrane scaffold remained unclear. Here, we elucidated the biosynthetic pathway of **2** and demonstrated that a novel TC is capable of directly generating **25** from FPP through Coates' route using isotopically sensitive branching coupled with mutagenesis studies.

Results and discussion

Identification and characterization of the biosynthetic genes of terrecyclic acid

To investigate the biosynthesis of **2**, we hypothesized that the biosynthetic genes should include not only a sesquiterpene cyclase as the core gene but also oxidases to generate the highly oxygenated scaffold of **2**. To locate these biosynthetic genes, the genome of the producer of **2** *Aspergillus terreus* ATCC 20516 was sequenced and analyzed. Three biosynthetic gene clusters (BGCs) were identified encoding both a TC and oxidative tailoring enzymes such as a cytochrome P450, α-ketoglutarate-dependent oxidase, or flavoenzyme (Fig. S1†). To further identify the BGC of **2**, we compared the differential gene expression of *A. terreus* ATCC 20516 before and after **2** was produced (Fig. S13†). Only one of the BGCs, a four-gene cassette on scaffold 58 was significantly upregulated during the production

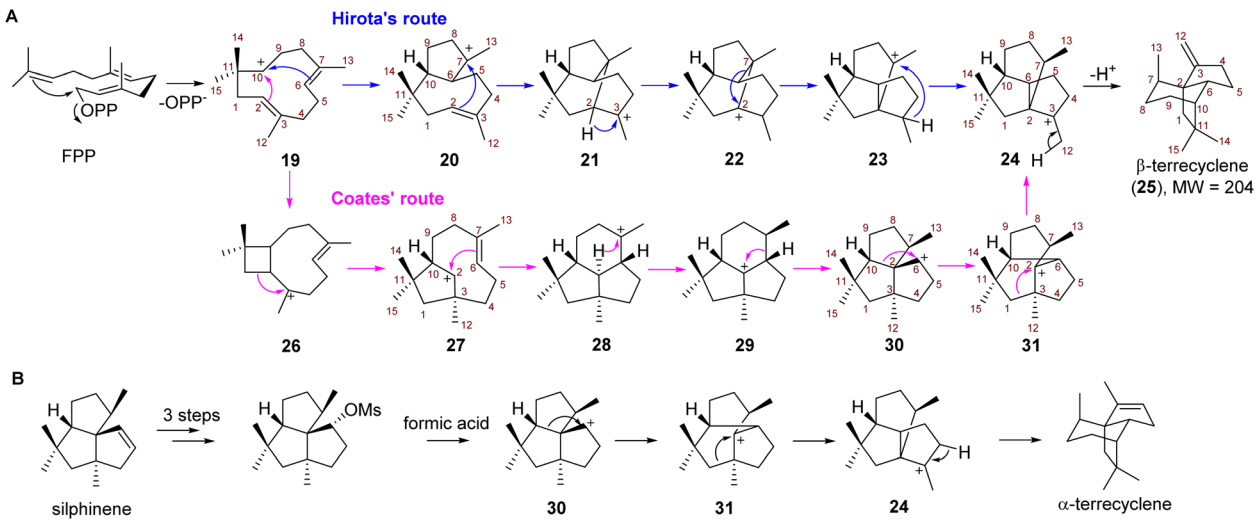

Scheme 1 The proposed mechanisms of β-terrecyclene formation. (A) Hirota's route (blue) and Coates' route (pink) to generate β-terrecyclene from farnesyl diphosphate (FPP). (B) Coates' rearrangement to form α-terrecyclene.

of **2**; this BGC contains a TC (*terA*), a cytochrome P450 (*terB*), a short-chain dehydrogenase/reductase (SDR, *terC*), and a transporter of the major facilitator superfamily (MFS, *terD*) (Fig. 2A and Table S5†).

To characterize the function of each gene in the BGC, intron-free *terA–C* were cloned from cDNA and heterologously expressed in *Saccharomyces cerevisiae* RC01, which was engineered to express the *A. terreus* electron transfer partner cytochrome P450 reductase.[17,18] The yeast cell expressing *terA* was able to produce a new sesquiterpene, which was determined to be **25** using NMR spectroscopy (Fig. 2B, S2 and Table S6†). When TerA was purified to homogeneity (Fig. S4†), **25** was also observed as the only product in the presence of 1 mM FPP and 5 mM $MgCl_2$ (Fig. 2B). To study the function of *terB* and *terC*, we attempted the heterologous expression of *terAB* and *terABC* in *S. cerevisiae* RC01. However, only a trace amount of new products with molecular weights of 250 and 248 were able to be detected possibly due to the low catalytic efficiency of the cytochrome P450 TerB in yeast (Fig. S5†). We then switched to another well-established eukaryotic host *Aspergillus nidulans* A1145.[19,20] When *terA* and *terB* were expressed in *A. nidulans*, the yield of the new products, with identical molecular weights and retention times, was dramatically increased. The new product with a molecular weight of 248 was characterized to be **2**, while the fractions with a molecular weight of 250 are **32** and **33**, respectively. All these products were characterized using NMR spectroscopy and X-ray crystallography (Fig. 2C, F, S2, S3 and Table S6†). When all three genes *terA–C* were co-expressed together, the yield of **2** was increased and only compound **33** was accumulated, which implied that **32** was possibly converted into **2** using TerC (Fig. 2C).

To identify the function of TerC, we expressed and purified the short-chain dehydrogenase/reductase in *Escherichia coli*. Biochemical analysis was performed using compounds **32** and **33** as substrates respectively. The oxidation of **32** into **2** was able to be catalyzed using TerC in the presence of the cofactor nicotinamide adenine dinucleotide phosphate ($NADP^+$), while the activity of boiled TerC was abolished (Fig. 2D). On the other hand, TerC failed to catalyze the oxidation of compound **33** into **2** using the $NADP^+$ cofactor, which indicated that only **32** is the substrate of TerC, while **33** is likely a shunt product derived from **2**. The reducing ability of TerC was then assessed in the presence of the cofactor NADPH using **2**, resulting in the exclusive formation of product **32**. This observation aligns with

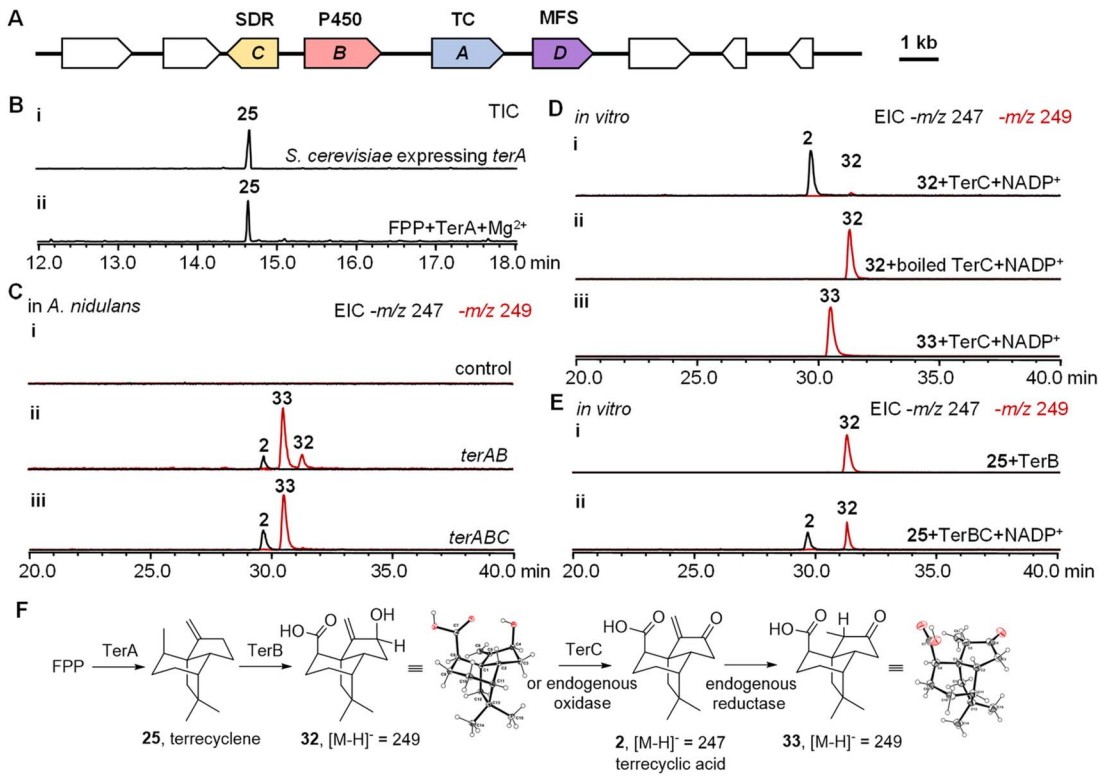

Fig. 2 Characterization of the biosynthetic pathway of terrecyclic acid. (A) Biosynthetic gene cluster of terrecyclic acid (**2**). The hypothetic proteins are in white. (B) Characterization of TerA using heterologous expression in *S. cerevisiae* (i) and *in vitro* biochemical analysis (ii). The total ion chromatograms (TICs) were obtained using GC-MS. (C) Heterologous expression of *ter* biosynthetic genes in *A. nidulans*: (i) *A. nidulans* carrying the empty vectors; (ii) *A. nidulans* carrying *terA* and *terB*; (iii) *A. nidulans* carrying *terA*, *terB*, and *terC*. The extracted ion chromatograms (EICs) were obtained using LC-MS. (D) *In vitro* characterization of TerC: (i) conversion of **32** into **2** catalyzed by TerC; (ii) boiled TerC abolishes the catalytic activity on substrate **32**; (iii) TerC is not able to catalyze the conversion of **33** into **2**. The EICs were obtained using LC-MS. (E) *In vitro* characterization of TerB: (i) conversion of **25** into **32** catalyzed by TerB; (ii) conversion of **25** into **2** catalyzed by TerB and TerC. (F) Proposed biosynthetic pathway of **2** and the related products. The EICs were obtained using LC-MS. The *Y*-axes of the chromatograms for each experiment are depicted on the same scale, ensuring comparable quantities of the compounds.

previous findings that TerC can catalyze the conversion of **32** back to **2** in the presence of $NADP^+$. Thus, it provides further evidence that **32** serves as a precursor to **2** (Fig. S6†). We therefore propose that *A. nidulans* A1145 possesses an isozyme of TerC which catalyzes the conversion of **32** into **2** at a low efficiency in the absence of TerC. Subsequently, an endogenous reductase in the host likely catalyzes the reduction of **2** to generate **33** (Fig. 2F). To validate our hypothesis, we conducted feeding experiments with compounds **2**, **32**, and **33** using the heterologous expression host. When **2** was fed to *A. nidulans* for 4 hours, it underwent conversion into **33** (Fig. S6A†). Conversely, feeding **32** to *A. nidulans* led to the generation of both **2** and **33** as products. However, no modified product was observed when **33** was fed to *A. nidulans* (Fig. S6A†). These findings indicate that **32** can be converted into **2** by an endogenous oxidase present in *A. nidulans*. Subsequently, **2** is further modified through the action of an endogenous reductase in *A. nidulans*, leading to the generation of **33** (Fig. 2F and S6B†).

To avoid modification of **32** and **2** by the endogenous enzymes, we performed *in vitro* biochemical analysis using the corresponding microsomal fractions of *A. nidulans* expressing *terB*. The sesquiterpene precursor **25** was successfully converted into a single oxidized product **32**, which could be further converted into a single product **2** using TerC (Fig. 2E). Thus the biosynthetic pathway of **2** could be proposed. First, TerA catalyzes the cyclization of FPP to give **25**, which is then iteratively oxidized by TerB to install the hydroxyl and carboxylic acid in **32**. Finally, dehydrogenation of **32** catalyzed by TerC takes place to generate **2** (Fig. 2F).

Mutagenesis studies of TerA

We next investigated the mechanism involved in carbocationic rearrangement during the formation of **25** catalyzed using TerA. To identify the key residues in the active site of TerA that are responsible for guiding the carbocationic intermediates to the quadrane scaffold, we predicted the three-dimensional structure of TerA using the Phyre 2 server.[21] Although the identity of the amino acid sequence is not very high between TerA and several representative sesquiterpene synthases including *epi*-isozizaene synthase,[22] selinadiene synthase,[23] and pentalenene synthase,[24] their overall three-dimensional structures are similar (Fig. S8 and S9†). To approximate the key residues in the active site that are responsible for binding and folding FPP, we aligned the predicted structure of TerA to selinadiene synthase complexed with substrate mimic 2,3-dihydro-FPP and Mg^{2+} (Fig. S10†). 10 residues lining the FPP binding pocket were identified, which included C111, V114, F115, D116, L120, F189, I219, Q260, W342 and S343 (Fig. 3A). To validate the prediction, alanine scanning was performed on these residues. The corresponding 10 TerA mutants were generated and heterologously produced in *S. cerevisiae* RC01. Analysis of the sesquiterpene product profile ($m/z = 204$) of the host expressing each mutant showed the mutations of F115A and W342A lead to almost complete loss of β-terrecyclene synthase activity (Fig. S11†). On the other hand, mutant V114A was capable of producing **25** as a major fraction, together with β-caryophyllene (**34**) and other unknown sesquiterpenes as minor fractions (Fig. 3B). However, the structure of the other minor fractions was not determined due to low yield. Interestingly, coproduct **34** could be derived *via* deprotonation of caryophyllenyl ion **26**, an intermediate proposed by Coates' route (Fig. 3C). This observation suggested the formation of β-terrecyclene is more likely through Coates' route.

To further investigate the catalytic functions of residues in the active site of TerA, we performed additional mutagenesis on these residues, substituting them with various amino acids other than alanine (Fig. S11†). We generated 21 TerA mutants and analyzed their product profiles. While most of the mutations decreased the terpene cyclase activity, they did not yield any new products. Their activities were similar to either the wild-type TerA or the corresponding alanine mutants. For instance, mutations of C111 to serine, tyrosine, and aspartate resulted in a reduction in the yield of **25** as the sole product. Mutation of F115 to other aromatic amino acids, such as tyrosine and tryptophan, resulted in a reduced yield of **25** compared to F115A. The F115W mutant also exhibited very low production of a few other sesquiterpenes, possibly due to improper folding

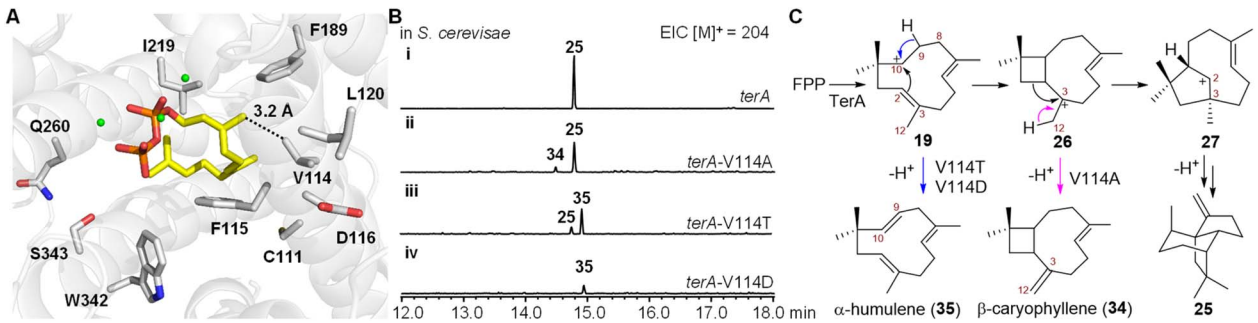

Fig. 3 Mutagenesis of TerA. (A) The predicted model of TerA with the key residues (grey) in the active site responsible for terrecyclene formation. The substrate mimic 2,3-dihydro-FPP is in yellow. The magnesium cation is in green. (B) Representative sesquiterpene product profile of *S. cerevisiae* expressing *terA* mutants: (i) *S. cerevisiae* expressing wildtype *terA*; (ii) *S. cerevisiae* expressing *terA*-V114A; (iii) *S. cerevisiae* expressing *terA*-V114T; (iv) *S. cerevisiae* expressing *terA*-V114D. The EICs were obtained using GC-MS. The *Y*-axes of the chromatograms for each experiment are depicted on the same scale, ensuring comparable quantities of the compounds. (C) The proposed mechanism of the formation of shunt products catalyzed by TerA mutants. **34** is derived from the key intermediate **26** in Coates' route (pink), while **35** is derived from the intermediate **19** in both Hirota's and Coates' routes (blue).

of the substrate FPP. Substituting the acidic residue aspartate at position 116 with glutamate or asparagine led to a decrease in the yield of **25**. The mutation of L120 to a smaller amino acid did not affect the yield of **25**, whereas the L120I mutation decreased production. Mutating F198 to aromatic residues, such as tyrosine and tryptophan, resulted in a decreased yield of **25**. Similarly, mutations of W342 to aromatic residues, such as tyrosine and phenylalanine, also led to a decrease in the production of **25**, and mutations of Q260 to asparagine and glutamate reduced the activity of TerA. When S343 was mutated to threonine, the production of **25** decreased. However, mutating S343 to phenylalanine completely abolished the catalytic activity of TerA. The hydrophobic residue V114 was mutated to a larger hydrophobic residue (leucine), an aromatic residue (phenylalanine), a polar residue (threonine), and an acidic residue (aspartate), respectively. Compared to V114A, both V114L and V114F mutants completely lost terpene cyclase activity, suggesting a strict size limitation for the residue at this position. On the other hand, mutants V114T and V114D produced a new compound, **35**, identified as α-humulene (Fig. 3B and S11†).

These results indicated that the structure of each residue located in the active sites of TerA is not strictly required for the generation of **25**. Except for V114, mutations of these residues do not dramatically switch the cyclization pathway to yield other shunt products. Intriguingly, **35** could be derived from intermediate **19**, forming a shunt product for both Hirota's and Coates' pathways (Fig. 3C). In the predicted model of the TerA active sites, residue V114 is close to the C12 of substrate mimic 2,3-dihydro-FPP (Fig. 3A). Therefore, we propose that the mutation of V114 to the smaller residue alanine enlarges the substrate binding pocket, leading to reduced selectivity of the 1,2-alkyl shift of **26**, and the concurrent generation of the C12 proton elimination product **34** (Fig. 3C). Additionally, the mutation of V114 to hydrogen bonding acceptor-containing residues may facilitate hydrogen abstraction at C9 of intermediate **19**, resulting in the formation of another shunt product **35** (Fig. 3C).

Isotopically sensitive branching reveals that the formation of β-terrecyclene follows Coates' route

Although the coproduction of **34** resulting from mutant V114A suggested the formation of β-terrecyclene is more likely through Coates' route, additional evidence would be needed to conclusively demonstrate that **26** is on the direct pathway to **25**. As a main distinction between Hirota's and Coates' routes, the formation of **26** could be validated using the well-established isotopically sensitive branching approach.[25–27] Therefore, we speculated that the substitution of all three protons on C12 of FPP by deuterium ([12-$^2H_3$]-FPP) would result in the decrease of the ratio of **34** to **25** produced by V114A mutant if the carbocation rearrangement is *via* the Coates' route (Scheme 1A and Fig. 4A). The production of **34** would be suppressed due to the primary deuterium kinetic isotope effect (KIE) on the deprotonation of **26** to yield **34** (Fig. 4A). On the other hand, the distribution of **34** and **25** would not be affected while using [12-$^2H_3$]-FPP as substrate, on the condition that cyclization follows Hirota's route (Fig. 4A).

Thus, recombinant TerA-V114A mutant was obtained upon heterologous expression in *S. cerevisiae* RC01 to perform the following *in vitro* analysis (Fig. S4†). In the presence of 1 mM FPP and 5 mM $MgCl_2$, TerA-V114A was able to convert FPP to a 1 : 4 mixture of coproducts **34** and **25** (Fig. 4B and S11†). When using [12-$^2H_3$]-FPP as a substrate at the same reaction condition, the ratio of **34** to **25** was significantly shifted to 1 : 10, with the ~53% decreased yield of **34** and ~18% increased production of **25** (Fig. 4B and S12†). The decreased ratio of **34** to **25** from 1 : 4 to 1 : 10 resulting from isotopically sensitive branching demonstrated that **26** is a common carbocation precursor to form both **34** and **25** (Fig. 4B). This indicated the cyclization of FPP to construct **25** is through Coates' route. Based on the shift of product distribution, the observed primary KIE on deprotonation of **26** to give **34** was determined to be $k_H/k_D = 2.5$. The magnitude of KIE is consistent with primary deuterium KIEs on similar terpene synthase-promoted methyl deprotonation, $k_H/k_D = 2$–6.[27–31]

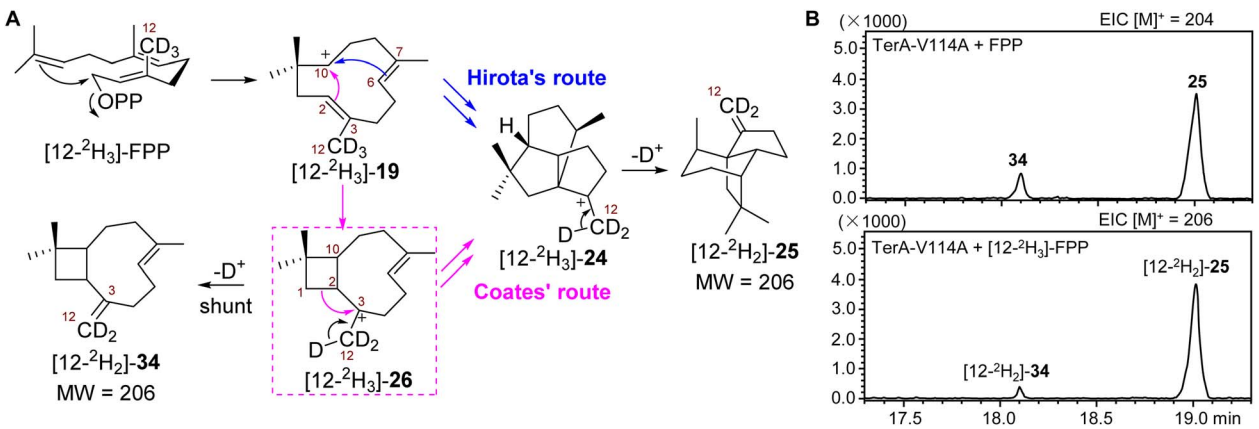

Fig. 4 Isotopically sensitive branching study of TerA-V114A mutant. (A) Distinguishing between Hirota's and Coates' routes through an isotopically sensitive branching experiment using [12-$^2H_3$]-FPP as substrate. (B) Effect of deuteration at C12 of FPP on the ratio of products generated by TerA-V114A. GC-MS chromatograms of reaction mixtures using FPP (top) and [12-$^2H_3$]-FPP (bottom). The EICs were obtained using GC-MS.

Conclusions

In summary, we elucidated the biosynthetic pathway of **2** *via* quadrane scaffold formation using the β-terrecyclene synthase and oxidative tailoring enzymes. The mechanism of enzymatic quadrane scaffold formation was demonstrated through mutagenesis and isotopically sensitive branching experiments, settling a decades-old mystery in the field of natural product biosynthesis. We propose that more natural products of the quadrane family can be identified using *ter* biosynthetic genes as a query to search in the public fungal genome database.

Data availability

Crystallographic data for compound **32** and **33** have been deposited at the CCDC under 2271713 and 2271714 respectively. The other datasets supporting this article have been uploaded as part of the ESI.†

Author contributions

Y. Y. and Y. T. designed the research. Y. S., W. W., J. Y., and S. W. performed the experiments. Y. S., Y. Y., Y. Z., J. B., D. G., J. W., and J. J. analyzed the data. Y. Y., Y. S., and J. B. wrote the manuscript. All the authors have approved the final version of the manuscript.

Conflicts of interest

There are no conflicts to declare.

Acknowledgements

This work was supported by the National Key Research and Development Program of China (2022YFC2805000, 2023YFA0914200); Hainan Provincial Joint Project of Sanya Yazhou Bay Science and Technology City (2021CXLH0013); the National Natural Science Foundation of China (32000044); Local Innovative and Research Teams Project of Guangdong Pearl River Talents Program (2019BT02Y262); K. C. Wong Education Foundation (GJTD-2020-12); Hainan Provincial Natural Science Foundation of China (823CXTD393); Key Science and Technology Plan Projects in Nansha District (2023ZD010). We are grateful to the analytical facilities in SCSIO for recording mass, NMR, and X-ray crystallography data.

Notes and references

1 D. W. Christianson, *Chem. Rev.*, 2017, **117**, 11570–11648.
2 J. D. Rudolf and C.-Y. Chang, *Nat. Prod. Rep.*, 2020, **37**, 425–463.
3 M. Presset, Y. Coquerel and J. Rodriguez, *Eur. J. Org Chem.*, 2010, **2010**, 2247–2260.
4 G. J. Calton, R. L. Ranieri and M. A. Espenshade, *J. Antibiot.*, 1978, **31**, 38–42.
5 R. L. Ranieri and G. J. Calton, *Tetrahedron Lett.*, 1978, **19**, 499–502.
6 M. Nakagawa, A. Hirota, H. Sakai and A. Isogai, *J. Antibiot.*, 1982, **35**, 778–782.
7 C. Peter, P. Geoffroy and M. Miesch, *Org. Biomol. Chem.*, 2018, **16**, 1381–1389.
8 Y. Ren, M. Presset, J. Godemert, N. Vanthuyne, J.-V. Naubron, M. Giorgi, J. Rodriguez and Y. Coquerel, *Chem. Commun.*, 2016, **52**, 6565–6568.
9 D. E. Cane, Y. G. Whittle and T.-C. Liang, *Tetrahedron Lett.*, 1984, **25**, 1119–1122.
10 A. Hirota, M. Nakagawa, H. Sakai and A. Isogai, *Agric. Biol. Chem.*, 1984, **48**, 835–837.
11 J. J. M. Beale, R. L. Chapman and J. P. N. Rosazza, *J. Antibiot.*, 1984, **37**, 1376–1381.
12 A. Hirota, M. Nakagawa, H. Sakai, A. Isogai, K. Furihata and H. Seto, *Tetrahedron Lett.*, 1985, **26**, 3845–3848.
13 D. E. Cane, Y. G. Whittle and T.-C. Liang, *Bioorg. Chem.*, 1986, **14**, 417–428.
14 R. M. Coates, J. Z. Ho, M. Klobus and L. Zhu, *J. Org. Chem.*, 1998, **63**, 9166–9176.
15 M. Klobus, L. Zhu and R. M. Coates, *J. Org. Chem.*, 1992, **57**, 4327–4329.
16 J. E. Barquera-Lozada and G. Cuevas, *J. Org. Chem.*, 2011, **76**, 1572–1577.
17 M.-C. Tang, H.-C. Lin, D. Li, Y. Zou, J. Li, W. Xu, R. A. Cacho, M. E. Hillenmeyer, N. K. Garg and Y. Tang, *J. Am. Chem. Soc.*, 2015, **137**, 13724–13727.
18 D. A. Yee, T. B. Kakule, W. Cheng, M. Chen, C. T. Y. Chong, Y. Hai, L. F. Hang, Y.-S. Hung, N. Liu, M. Ohashi, I. C. Okorafor, Y. Song, M. Tang, Z. Zhang and Y. Tang, *J. Am. Chem. Soc.*, 2020, **142**, 710–714.
19 N. Liu, Y.-S. Hung, S.-S. Gao, L. Hang, Y. Zou, Y.-H. Chooi and Y. Tang, *Org. Lett.*, 2017, **19**, 3560–3563.
20 Z. Sun, C. S. Jamieson, M. Ohashi, K. N. Houk and Y. Tang, *Nat. Commun.*, 2022, **13**, 2568.
21 L. A. Kelley, S. Mezulis, C. M. Yates, M. N. Wass and M. J. E. Sternberg, *Nat. Protoc.*, 2015, **10**, 845–858.
22 P. N. Blank, G. H. Barrow, W. K. W. Chou, L. Duan, D. E. Cane and D. W. Christianson, *Biochemistry*, 2017, **56**, 5798–5811.
23 P. Baer, P. Rabe, K. Fischer, C. A. Citron, T. A. Klapschinski, M. Groll and J. S. Dickschat, *Angew. Chem., Int. Ed.*, 2014, **53**, 7652–7656.
24 C. A. Lesburg, G. Zhai, D. E. Cane and D. W. Christianson, *Science*, 1997, **277**, 1820–1824.
25 L. Zu, M. Xu, M. W. Lodewyk, D. E. Cane, R. J. Peters and D. J. Tantillo, *J. Am. Chem. Soc.*, 2012, **134**, 11369–11371.
26 X. He and D. E. Cane, *J. Am. Chem. Soc.*, 2004, **126**, 2678–2679.
27 D. J. Schenk, C. M. Starks, K. R. Manna, J. Chappell, J. P. Noel and R. M. Coates, *Arch. Biochem. Biophys.*, 2006, **448**, 31–44.
28 K. Wagschal, T. J. Savage and R. Croteau, *Tetrahedron*, 1991, **47**, 5933–5944.
29 R. B. Croteau, C. J. Wheeler, D. E. Cane, R. Ebert and H. J. Ha, *Biochemistry*, 1987, **26**, 5383–5389.
30 H. J. Pyun, R. M. Coates, K. C. Wagschal, P. McGeady and R. B. Croteau, *J. Org. Chem.*, 1993, **58**, 3998–4009.
31 K. C. Wagschal, H. J. Pyun, R. M. Coates and R. Croteau, *Arch. Biochem. Biophys.*, 1994, **308**, 477–487.